Neuro-Oncology
21(11), 1423–1435, 2019 | doi:10.1093/neuonc/noz107 | Advance Access date 21 June 2019

Targeting PDGFRα-activated glioblastoma through specific inhibition of SHP-2–mediated signaling

Youzhou Sang,[#] Yanli Hou,[#] Rongrong Cheng, Liang Zheng, Angel A. Alvarez, Bo Hu, Shi-Yuan Cheng, Weiwei Zhang, Yanxin Li, and Haizhong Feng

State Key Laboratory of Oncogenes and Related Genes, Renji-Med X Clinical Stem Cell Research Center, Ren Ji Hospital, Shanghai Cancer Institute, School of Medicine, Shanghai Jiao Tong University, Shanghai, China (Y.S., W.Z., H.F.); Department of Radiotherapy, Ren Ji Hospital, School of Medicine, Shanghai Jiao Tong University, Shanghai, China (Y.H.); Key Laboratory of Pediatric Hematology and Oncology Ministry of Health, Pediatric Translational Medicine Institute, Shanghai Children's Medical Center, School of Medicine, Shanghai Jiao Tong University, Shanghai, China (R.C., L.Z., Y.L.); The Ken and Ruth Davee Department of Neurology, Lou & Jean Malnati Brain Tumor Institute, The Robert H. Lurie Comprehensive Cancer Center, Northwestern University Feinberg School of Medicine, Chicago, Illinois, USA (A.A.A., B.H., S-Y.C.)

Corresponding Author: Haizhong Feng, Ph.D. or Weiwei Zhang, Ph.D., State Key Laboratory of Oncogenes and Related Genes, Renji-Med X Clinical Stem Cell Research Center, Ren Ji Hospital, or Yanxin Li, Ph.D., Key Laboratory of Pediatric Hematology and Oncology Ministry of Health, Shanghai Children's Medical Center, School of Medicine, Shanghai Jiao Tong University, Shanghai, 200127, China (fenghaizhong@sjtu.edu.cn), (liyanxincau@163.com), or (zhangweiw1980@126.com)

[#]These authors equally contributed to this work.

Abstract

Background. Glioblastoma (GBM) is the most malignant primary brain tumor, with dismal median survival. Treatment of GBM is particularly challenging given the intrinsic resistance to chemotherapy and difficulty of drugs to reach the tumor beds due to the blood–brain barrier. Here, we examined the efficacy of SHP099, a potent, selective, and oral SHP-2 inhibitor for treating GBM with activated platelet derived growth factor receptor alpha (PDGFRα) signaling.

Methods. The effects of SHP099 on cell survival of neural progenitor cells (NPCs), GBM cell lines, and patient-derived glioma stem-like cells (GSCs) were evaluated. Brain and plasma pharmacokinetics of SHP099 and its ability to inhibit SHP-2 signaling were assessed. SHP099 efficacy as a single agent or in combination with temozolomide (TMZ) was assessed using transformed mouse astrocyte and GSC orthotopic xenograft models.

Results. Activated PDGFRα signaling in established GBM cells, GSCs, and transformed mouse astrocytes was significantly inhibited by SHP099 compared with NPCs in vitro and in vivo through targeting SHP-2–stimulated activation of extracellular signal-regulated protein kinases 1 and 2 in GBM. SHP099 treatment specifically inhibited expression of *JUN*, a downstream effector of PDGFR signaling, thereby attenuating cell cycle progression in GBM cells with activated PDGFRα. Moreover, SHP099 accumulated at efficacious concentrations in the brain and effectively inhibited orthotopic GBM tumor xenograft growth. SHP099 exhibited antitumor activity either as a single agent or in combination with TMZ and provided significant survival benefits for GBM tumor xenograft-bearing animals.

Conclusions. Our data demonstrate the utility and feasibility of SHP099 as a potential therapeutic option for improving the clinical treatment of GBM in combination with TMZ.

Key Points

1. GBM and GSC cells with PDGFRα activation are responsive to SHP099.
2. SHP099 accumulates at efficacious concentrations in the brain of immunocompetent animals.
3. SHP099 exhibits antitumor activity either as a single agent or in combination with TMZ.

© The Author(s) 2019. Published by Oxford University Press on behalf of the Society for Neuro-Oncology. All rights reserved.
For permissions, please e-mail: journals.permissions@oup.com

Importance of the Study

SHP-2 is a nonreceptor protein tyrosine phosphatase encoded by the *PTPN11* gene that is critical for PDGFRα-driven gliomagenesis. SHP099, a novel and potent SHP-2 inhibitor, preferentially attenuated cell survival and self-renewal of GSCs compared with neural progenitor cells in vitro. Delivered orally, SHP099 accumulated at efficacious concentrations in the brain, as determined using 2 different orthotopic xenograft models. SHP099 (as a single agent or in combination with the first-line chemotherapy, TMZ) inhibited tumor growth and extended survival of animals bearing xenografts with activated PDGFRα signaling. Therefore, SHP099 may serve as a treatment of clinical GBM in combination with TMZ.

Glioblastoma (GBM) is the most common malignant primary brain tumor in adults, with a 14.6-month median survival after diagnosis.[1,2] Small-molecule inhibitors hold therapeutic promise for treating GBM through perturbing autophagic activity of glioma stem-like cells (GSCs),[3] energy metabolism,[4] cell proliferation,[5] and cell signaling[6] in GBM tumor xenografts. However, clinical selection of effective therapeutic drugs for GBM treatment is limited. Thus, there is an urgent unmet need to identify new targets for developing effective therapeutic strategies against GBM.

SHP-2 is a nonreceptor protein tyrosine phosphatase (PTP) encoded by the *PTPN11* gene[7] and regulates multiple biological functions in response to various growth factors, hormones, or cytokines.[8,9] SHP-2 is critical for Ras/mitogen-activated protein kinase signaling–mediated cell survival, proliferation, migration, and differentiation.[10] Mutation, amplification, or aberrant activation of SHP-2 causes various diseases and cancers.[8,11] In glioma, inhibition of SHP-2 suppressed orthotopic GBM growth in NOD/SCID mice and decelerated the progression from low-grade astrocytoma to GBM in a mouse model of spontaneous transgenic glioma.[12] We have previously reported that SHP-2 promotes platelet derived growth factor receptor alpha (PDGFRα)–driven gliomagenesis with *Ink4a/Arf* deletion[13] and glioma cell epithelial-mesenchymal transition.[14]

Of note, approximately 13% of clinical GBMs harbor *PDGFRA* amplification[15,16] and SHP-2 mediates oncogenic PDGFRα signaling in cancers, including GBM.[13,14,17] Therefore, specific targeting of SHP-2 by novel inhibitors is expected to help to develop an effective therapy for GBM with PDGFRα activation. Recently an allosteric SHP-2 inhibitor, SHP099, was characterized as a potent and highly specific inhibitor of SHP-2. SHP099 effectively diminishes activation of extracellular signal-regulated kinase 1 and 2 (ERK1/2) and proliferation of cancer cells driven by receptor tyrosine kinases (RTKs)[18,19] or *KRAS* alterations.[20–23] Moreover, SHP099 prevents adaptive resistance to MEK inhibitors in multiple types of human cancers.[20–23]

Here, we investigated whether SHP099 is a potent inhibitor in gliomas with activated PDGFRα signaling. We determined the response to SHP099 in GSCs and the pharmacokinetics of SHP099 in brain tissues and plasma of immunocompetent mice. Treatment with SHP099 either as a single agent or in combination with temozolomide (TMZ) was then performed.

Materials and Methods

Cell Lines

Neural progenitor cells (NPCs) and GL261 were purchased from American Type Culture Collection. The LN444 glioma cell line was a gift from Dr Erwin G. Van Meir at Emory University. Patient-derived GSC lines—1123, R83, R39, 528, 157, and AC17—were from Dr Ichiro Nakano[24] or our collections. Molecular subtype, O^6-methylguanine-DNA methyltransferase methylation status, and isocitrate dehydrogenase 1 mutations identified for each patient-derived GSC line are shown in Supplementary Table 1. Primary *Ink4a/Arf*$^{-/-}$ mouse astrocytes (mAsts) were derived and propagated as previously described.[25]

Chemicals

SHP099 ($C_{16}H_{19}Cl_2N_5$, molecular weight: 355.26; #HY-100388) and TMZ (HY-17364) were purchased from MedChemExpress and dissolved in double-distilled (dd) H_2O.

Plasmids

PDGF-A and PDGFRα constructs were derived as we previously described.[13] SHP-2 short hairpin (sh)RNAs and control shRNAs were purchased from Shanghai GeneChem Company.

Cell Viability Assays

Cell viability analysis was performed using a WST-1 assay kit (Roche). Briefly, cells were seeded in triplicate wells of a 96-well microplate (6000 cells/well) and treated with vehicle (ddH_2O) or SHP099 from 0.1 to 100 μM for 72 hours. Half-maximal inhibitory concentration (IC_{50}) values were calculated from fitted concentration-response curves obtained from at least 3 independent experiments.

Colony Formation and Limiting Dilution Glioma Sphere-Forming Assays

Colony formation assay and limiting dilution assays were performed as we previously described.[26] The

sphere-forming frequency of patient-derived GSCs was calculated as described in http://bioinf.wehi.edu.au/software/elda/.

Cell Cycle and Apoptosis Assays

These assays were performed using flow cytometry as we previously described.[20]

RNA Isolation, RNA Sequencing, and Gene Set Enrichment Analysis

RNA isolation and RNA-Seq analysis were performed as we previously described.[26] Gene set enrichment analysis (GSEA) was performed with the javaGSEA Desktop Application by using 1000 gene set permutations, the provided Gene Ontology biological process and transcription factor motif gene sets, and all other default settings.[27] RNA-Seq data reported in this study have been deposited with the Gene Expression Omnibus under accession ID GSE126892.

Pharmacokinetics of SHP099

C57BL/6J female mice aged 6–8 weeks (Shanghai Laboratory Animal Center) were administered by oral gavage with a single dose of SHP099 (100 mg/kg in a total volume of 400 μL). Afterward, the brain tissues and plasma were harvested at indicated time points post oral gavage (0 min, 30 min, 1 h, 2 h, 4 h, 8 h, and 24 h), lysed, and analyzed by ultra high performance liquid chromatography/mass spectroscopy (UHPLC-MS; Thermo Scientific, UPLC with Q Exactive Plus mass spectrometer) as described previously.[19] We used 2-amino-5-phenylpyrazine (Sigma 13535-13-2) as an internal standard of SHP099. More details are described in the Supplementary Methods.

Tumorigenicity Studies

Tumorigenicity studies were performed as we previously described[26] (see details in the Supplementary Methods). All animal experiments were approved by the Shanghai Jiao Tong University Institutional Animal Care and Use Committee.

Western blotting, quantitative reverse transcriptase (qRT)-PCR, shRNA knockdown and transfection, and immunohistochemistry (IHC) assays. These assays were performed as previously described[26] (see details in the Supplementary Methods and Supplementary Table 2).

Statistical Analysis

All statistical analyses were performed using GraphPad Prism 5 software. A minimum of 2 or 3 independent biological replicates were analyzed using Student's *t*-test (two-tailed) or one-way ANOVA (Newman–Keuls post hoc test) as specified in the Figure legends. Data are means ± SD of 3 independent experiments. Survival analysis was performed using Kaplan–Meier analysis and the log-rank test. $P < 0.05$ was considered significant.

Results

GSCs Are More Responsive to SHP099 Treatments

SHP099 is a potent, selective, orally available SHP-2 inhibitor with IC_{50} of 70 nM in vitro, and is known to inhibit cell proliferation in several solid and hematologic malignancies at various IC_{50} values ranging from 0.03 to over 30 μM.[18] Orally administered SHP099 shows dose-dependent antitumor activity in an esophageal squamous cell carcinoma KYSE-520 xenograft mouse model and is well tolerated up to 100 mg/kg.[18] To assess the effects of SHP099 on glioma cells, we performed cell viability analysis and found that compared with NPCs, patient-derived GSCs 1123, R83, R39, 528, 157, and AC17 were more sensitive to SHP099 (Figure 1A and 1B). SHP099 markedly inhibited glioma sphere formation in GSC R83, R39, and 157 cells (Figure 1C). To investigate the reason that all GSCs were more responsive to SHP099 than NPCs, we assessed expression of epidermal growth factor receptor (EGFR) and PDGFRα, 2 important RTK drivers in gliomagenesis.[15,28] EGFR or its mutant, variant III (EGFRvIII), was highly expressed in GSC 1123, R83, and R39 cells with high EGFR phosphorylation (p-EGFR), while PDGFRα and p-PDGFRα were highly expressed in GSC 528, 157, and AC17 cells (Figure 1D). Although SHP-2 protein levels were similar in all GSCs compared with NPCs, p-SHP-2 levels were higher in GSCs (Figure 1D). These data indicated that the selective inhibition of GSCs by SHP099 is dependent on hyperactivated RTKs.

Glioma Cells with PDGFRα Activation Are Highly Responsive to SHP099

Since we previously reported that SHP-2 is highly important for PDGFRα-driven glioma tumorigenicity,[13] we further determined whether glioma cells with aberrant activation of PDGFRα are more responsive to SHP099. As shown in Figure 2A and Figure 1D, PDGF-A stimulation markedly promoted SHP099 responses in GSC 157 and AC17 cells with activated PDGFRα signaling but not in GSC 1123 and R83 cells with minimal or no PDGFRα activation.

We validated this effect in LN444 GBM cells and *Ink4a/Arf*$^{-/-}$ mAsts that were responsive to PDGF-A stimulation.[13,29] As shown in Figure 2B–D, compared with the empty vector (EV) control, SHP099 markedly inhibited cell viability in LN444 GBM cells overexpressing PDGF-A, which featured high PDGFRα activation and tumorigenicity as we previously described.[13,29] In addition, SHP099 significantly inhibited colony formation of LN444 cells with PDGF-A overexpression compared with the control (Figure 2E, F). Compared with *Ink4a/Arf*$^{-/-}$ mAst control, SHP099 markedly inhibited cell survival (Figure 2G–I) and colony formation (Figure 2J, K) in *Ink4a/Arf*$^{-/-}$ mAsts that overexpressed PDGFRα and PDGF-A and were highly tumorigenic in the mouse brain.[13] These data indicate that glioma cells with

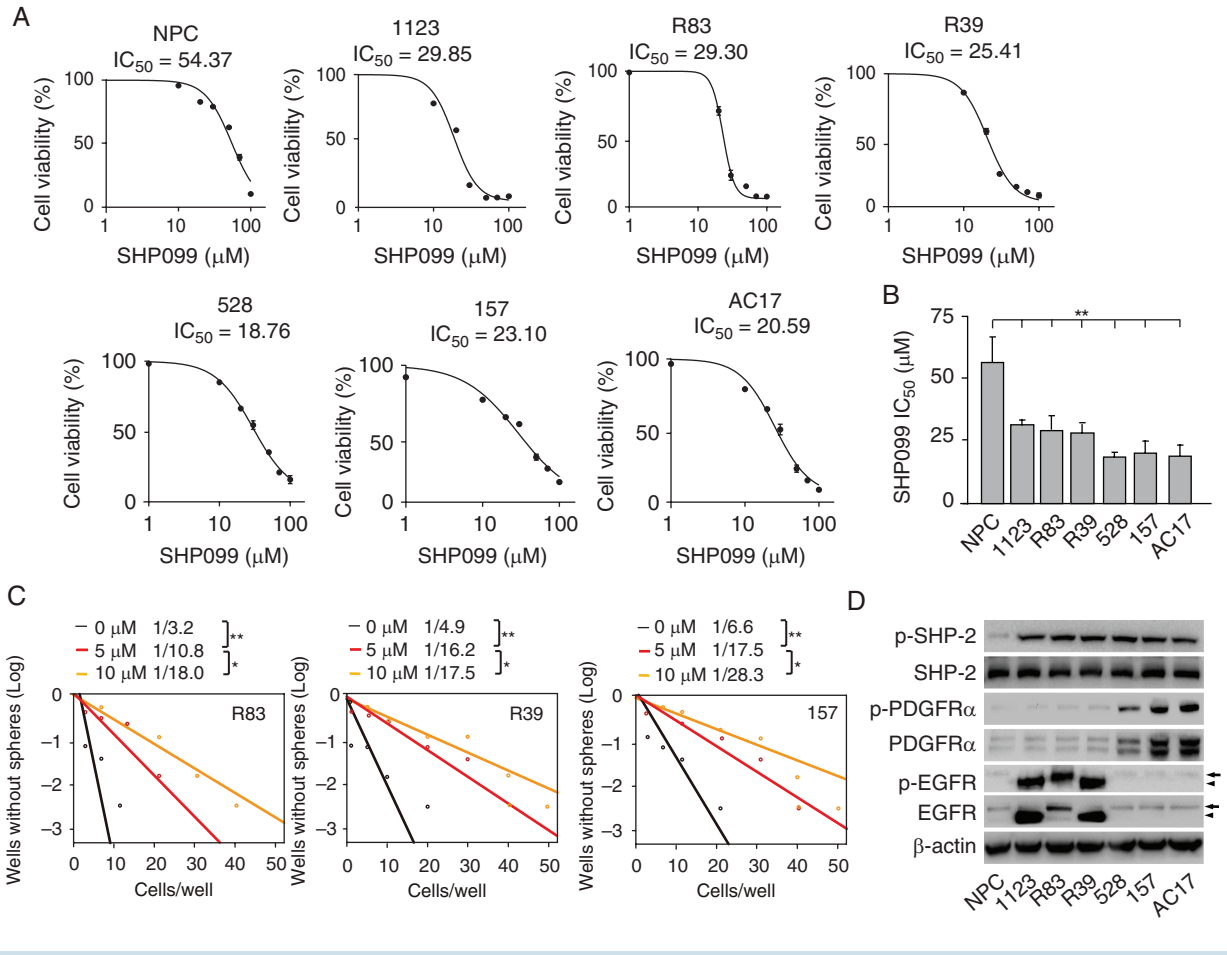

Fig. 1 GSCs are more responsive to SHP099 treatment than NPCs. (A) Viability of NPC, GSC 1123, R83, R39, 528, 157, and AC17 cells at 72 h after treatment with SHP099. (B) Comparison of SHP099 IC_{50} values in A. (C) Effects of SHP099 in limiting dilution glioma sphere-forming assay of GSC R83, R39, and 157 cells. (D) Western blotting (WB) analysis of expression levels of EGFR, p-EGFR, PDGFRα, p-PDGFRα, SHP-2, and p-SHP-2 in NPCs and GSCs. β-actin was used as a loading control. Arrow, EGFR; arrowhead, EGFRvIII. $^{*}P < 0.05$, $^{**}P < 0.01$, by one-way ANOVA.

activation of PDGFRα signaling yield better responses to SHP099 treatment.

SHP099 Specifically Inhibits PDGFRα-SHP-2-Stimulated ERK1/2 Activity

SHP099 is an allosteric SHP-2 phosphatase inhibitor and inhibits ERK1/2 activation in cancer cells.[18,19] Thus, we determined whether SHP099 inhibits PDGFRα downstream SHP-2 activation in glioma cells. Consistent with our previous report,[13] PDGF-A stimulation moderately promoted p-PDGFRα and PDGFRα downstream phosphorylation of ERK1/2 and Akt in *Ink4a/Arf*$^{-/-}$ mAsts with an EV control compared with unstimulated cells (Figure 3A). Ectopic expression of PDGFRα wild-type (WT) but not receptor kinase-dead mutant (R627) further promoted PDGFRα phosphorylation and PDGFRα downstream phosphorylation of ERK1/2 and Akt in *Ink4a/Arf*$^{-/-}$ mAsts with PDGF-A stimulation (Figure 3A). SHP099 significantly inhibited PDGF-A–stimulated ERK1/2 phosphorylation (p-ERK1/2) (Figure 3A) and cell proliferation (Figure 3B) but not Akt phosphorylation (p-Akt) in *Ink4a/Arf*$^{-/-}$ mAsts with an EV or PDGFRα WT (Figure 3A) compared with the unstimulated cells, respectively. SHP099 had no effects on p-ERK1/2 and p-Akt (Figure 3A), and cell proliferation (Figure 3B) in cells expressing PDGFRα R627 mutant with or without PDGF-A stimulation.

Using genetic and biochemical methods, we and other investigators have described the roles of various tyrosine-to-phenylalanine (Y-to-F) mutations of PDGFRα on PDGFRα-regulated cellular functions and tumorigenesis.[13,30,31] To further determine whether SHP099 specifically inhibits PDGFRα-mediated SHP-2 activation, we separately expressed various PDGFRα mutants (with a specific deficiency in their downstream signaling) in *Ink4a/Arf*$^{-/-}$ mAsts as we previously described.[13] As shown in Figure 3C and 3D, compared with WT PDGFRα, ectopic expression of PDGFRα Y-to-F mutation at Y720 (F720, deficient for SHP-2

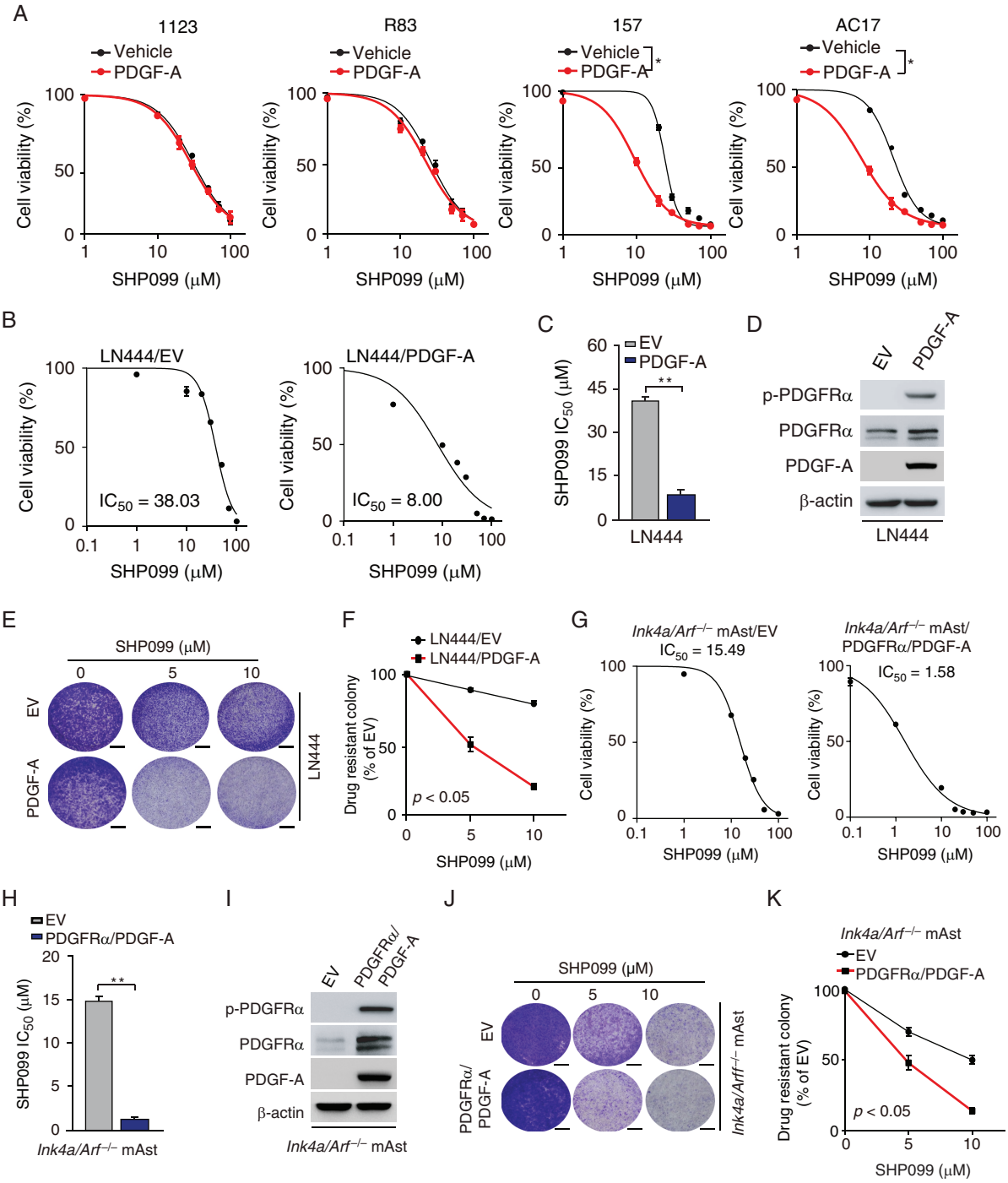

Fig. 2 Glioma cells with PDGFRα activation are more responsive to SHP099. (A) Viability of GSC 1123, R83, 157, and AC17 cells with PDGF-A stimulation after SHP099 treatment. GSCs were pre-cultured for 24 h in Dulbecco's modified Eagle's medium/F12 with EGF (2 ng/mL) and basic fibroblast growth factor (2 ng/mL) and then followed by co-culturing with or without 100 ng/mL PDGF-A and the indicated SHP099 concentrations for 72 h. (B and G) Viability of LN444 cells with ectopic expression of an EV or PDGF-A (B) or *Ink4a/Arf*$^{-/-}$ mAsts with overexpression of an EV or PDGFRα plus PDGF-A (G) at 72 h after treatment with SHP099. (C and H) Comparison of SHP099 IC_{50} in (B) or (G). (D and I) WB assays of expression of PDGF-A, PDGFRα, and p-PDGFRα in LN444 or *Ink4a/Arf*$^{-/-}$ mAsts. (E and J) Representative images of drug-resistant colony formation in LN444 cells (E) or *Ink4a/Arf*$^{-/-}$ mAsts (J) at day 7 post SHP099 treatment. (F and K) Quantification of drug-resistant colony formation in (E) and (J), respectively. Scale bars, 400 μm. $^{*}P < 0.05$, $^{**}P < 0.01$, by one-way ANOVA or two-tailed Student's *t*-test.

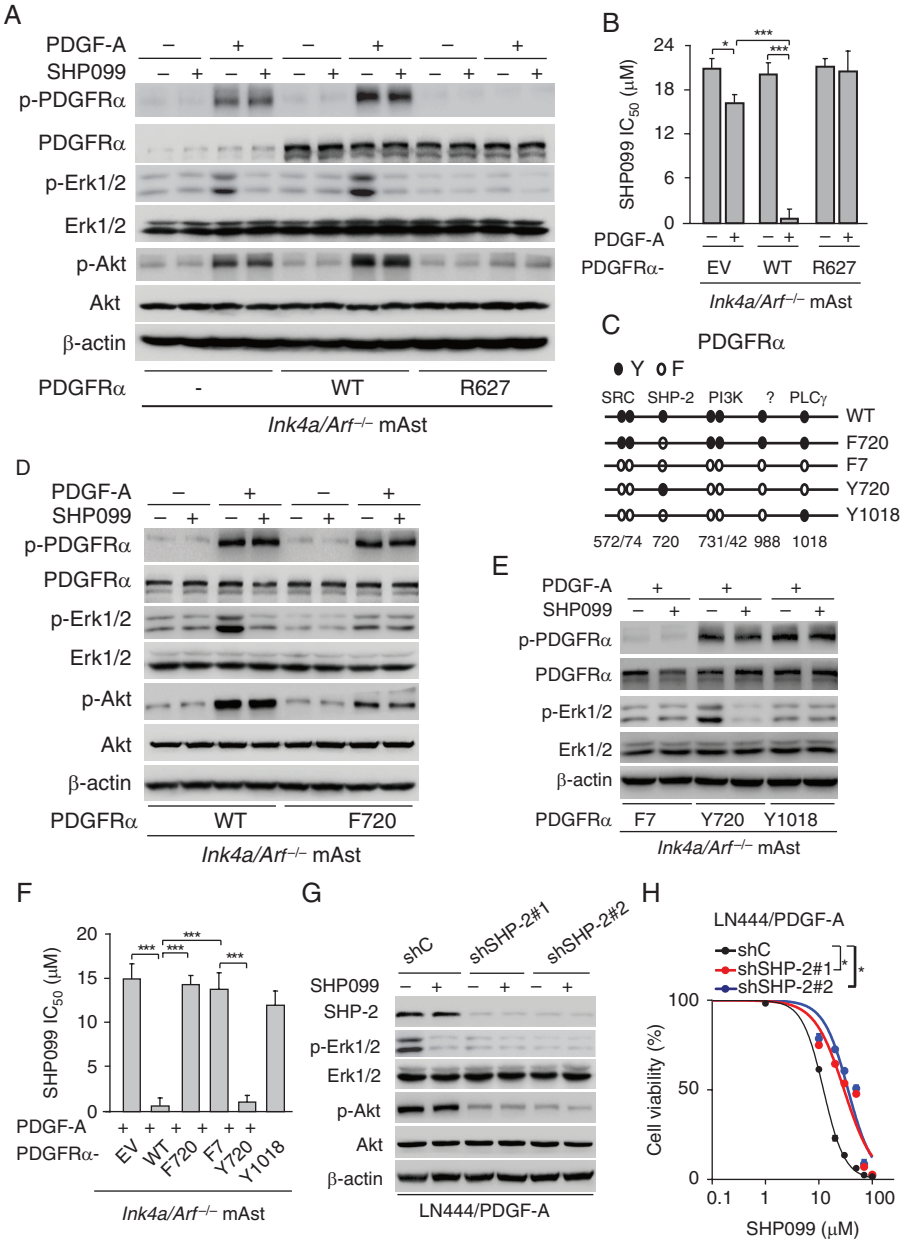

Fig. 3 SHP099 specifically inhibits PDGFRα–SHP-2-stimulated ERK1/2 activity. (A) WB assays of effects of SHP099 on PDGF-A stimulated p-PDGFRα, ERK1/2 phosphorylation (p-ERK1/2), and Akt phosphorylation (p-Akt) in *Ink4a/Arf*$^{-/-}$ mAsts overexpressing an EV, PDGFRα wild-type (WT), or kinase-dead mutant (R627). (B) Viability of *Ink4a/Arf*$^{-/-}$ mAsts with an EV, PDGFRα WT, or R627 mutant at 72 h after treatment with SHP099 in combination with or without PDGF-A stimulation. (C) Schematics of various PDGFRα mutants. (D) Effects of ectopic expression of PDGFRα WT and F720 mutant on SHP099 inhibition of ERK1/2 phosphorylation in *Ink4a/Arf*$^{-/-}$ mAsts. (E) Effects of expression of PDGFRα F7, Y720, and Y1018 mutants on SHP099 inhibition of ERK1/2 phosphorylation. (F) Viability of PDGF-A-stimulated *Ink4a/Arf*$^{-/-}$ mAsts with ectopic expression of an EV, PDGFRα WT, or indicated mutants at 72 h after treatment with SHP099. (G) Effects of SHP-2 knockdown on SHP099 inhibition of ERK1/2 phosphorylation in LN444 with PDGF-A overexpression. (H) Viability of LN444/PDGF-A/shSHP-2 and LN444/PDGF-A/shC cells at 72 h after treatment with SHP099. ShSHP-2, SHP-2 shRNAs. shC, a control shRNA. *$P < 0.05$, **$P < 0.01$, ***$P < 0.001$, by one-way ANOVA or two-tailed Student's *t*-test.

binding) attenuated PDGF-A–stimulated p-ERK1/2 and p-Akt (Figure 3D) and SHP099 responses (Figure 3F). However, SHP099 did not affect F720-inhibited p-ERK1/2 and p-Akt (Figure 3D) with or without PDGF-A stimulation. As we previously reported,[13] mAsts expressing PDGFRα-F7 mutant (harboring 7 Y-to-F mutations, including Y572/74F, Y720F, Y731/42F, Y988F, and Y1018F) abrogated PDGF-A stimulation of

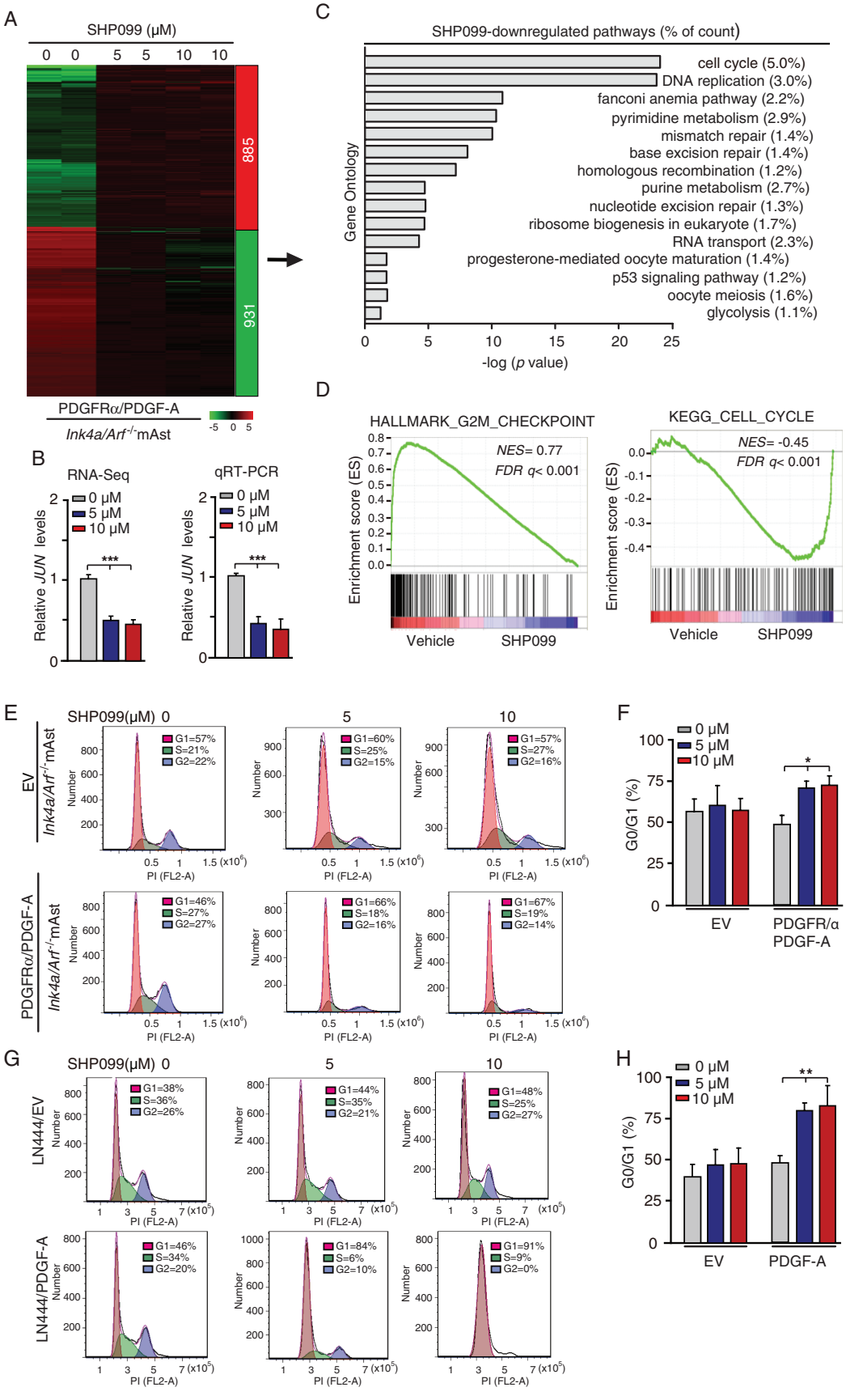
A
SHP099 (μM)
0 0 5 5 10 10
885
931
PDGFRα/PDGF-A
Ink4a/Arf-/- mAst
-5 0 5
B
RNA-Seq
qRT-PCR
0 μM
5 μM
10 μM
Relative JUN levels
***
C
SHP099-downregulated pathways (% of count)
cell cycle (5.0%)
DNA replication (3.0%)
fanconi anemia pathway (2.2%)
pyrimidine metabolism (2.9%)
mismatch repair (1.4%)
base excision repair (1.4%)
homologous recombination (1.2%)
purine metabolism (2.7%)
nucleotide excision repair (1.3%)
ribosome biogenesis in eukaryote (1.7%)
RNA transport (2.3%)
progesterone-mediated oocyte maturation (1.4%)
p53 signaling pathway (1.2%)
oocyte meiosis (1.6%)
glycolysis (1.1%)
Gene Ontology
-log (p value)
D
HALLMARK_G2M_CHECKPOINT
NES= 0.77
FDR q< 0.001
KEGG_CELL_CYCLE
NES= -0.45
FDR q< 0.001
Enrichment score (ES)
Vehicle
SHP099
E
SHP099(μM) 0
5
10
EV
Ink4a/Arf-/- mAst
PDGFRα/PDGF-A
G1=57%
S=21%
G2=22%
G1=60%
S=25%
G2=15%
G1=57%
S=27%
G2=16%
G1=46%
S=27%
G2=27%
G1=66%
S=18%
G2=16%
G1=67%
S=19%
G2=14%
Number
PI (FL2-A)
F
0 μM
5 μM
10 μM
G0/G1 (%)
*
EV
PDGFRα
PDGF-A
G
LN444/EV
LN444/PDGF-A
G1=38%
S=36%
G2=26%
G1=44%
S=35%
G2=21%
G1=48%
S=25%
G2=27%
G1=46%
S=34%
G2=20%
G1=84%
S=6%
G2=10%
G1=91%
S=9%
G2=0%
H
**

PDGFRα phosphorylation and p-ERK1/2 (Figure 3E). Reexpression of exogenous PDGFRα Y720 (SHP-2 binding site) but not Y1018 (phospholipase C gamma binding site) mutant in F7 PDGFRα mutant-expressing mAsts restored p-ERK1/2 (Figure 3E) and SHP099 responses (Figure 3F) with PDGF-A stimulation. However, SHP099 diminished PDGFRα-Y720 mutant-restored p-ERK1/2 (Figure 3E), whereas SHP099 exerted no effects on p-ERK1/2 (Figure 3E) in F7 PDGFRα mAsts after reexpressing the PDGFRα-Y1018 mutant. Additionally, consistent with our previous report,[13] in LN444 GBM cells with high endogenous expression of PDGFRα and stable expression of exogenous PDGF-A, knockdown of SHP-2 inhibited PDGF-A–stimulated p-ERK1/2 and p-Akt (Figure 3G). SHP099 inhibited p-ERK1/2 but not p-Akt in LN444/PDGF-A GBM cells and had no effects on SHP-2 shRNA–inhibited p-ERK1/2 and p-Akt (Figure 3G). SHP-2 knockdown rendered LN444/PDGF-A GBM cells unresponsive to SHP099 inhibition (Figure 3H). These results suggest that SHP099 specifically inhibits PDGFRα-mediated SHP-2 activity.

SHP099 Specifically Inhibits Cell Cycle Pathways in Gliomas with PDGFRα Activation

To understand the underlying mechanism by which glioma cells with activated PDGFRα signaling are more responsive to SHP099 treatment, we performed RNA-Seq analysis in *Ink4a/Arf*$^{-/-}$ mAsts with stable expression of PDGFRα and PDGF-A treated with or without SHP099. Gene expression profile analysis identified 885 genes whose expression was markedly increased by SHP099 and 931 genes whose expression was significantly reduced by SHP099 (fold change >2, $P < 0.05$) (Figure 4A). We further investigated the expression change of genes in the PDGFR signaling pathway, and found that expression levels of *JUN* were significantly inhibited by both 5 μM and 10 μM SHP099 treatment (Figure 4B). We further validated these results by qRT-PCR (Figure 4B).

The *JUN* gene encodes the c-JUN protein, which is a component of transcription factor AP-1 and is required for progression through the G1 phase of the cell cycle.[32] Accordingly, we performed Gene Ontology analysis and revealed that these SHP099- downregulated genes were mainly associated with cell cycle pathways, such as *CCND1*, *CCNE1*, and *CCNE2* (Figure 4C and Supplementary Figure 1). GSEA showed that cell cycle gene signatures were significantly altered in SHP099-treated *Ink4a/Arf*$^{-/-}$ mAsts (Figure 4D). Additionally, we evaluated the effects of SHP099 on expression levels of *CCND1*, *CCNE1*, and *CCNE2* by qRT-PCR in *Ink4a/Arf*$^{-/-}$ mAsts with or without PDGFRα/PDGF-A. As shown in Supplementary Figure 1, SHP099 treatment reduced the expression of *CCND1*, *CCNE1*, and *CCNE2* in *Ink4a/Arf*$^{-/-}$ mAsts with PDGFRα/PDGF-A but not the EV control.

To validate the SHP099-mediated regulation of the cell cycle in GBM cells, we performed cell cycle analysis using flow cytometry. As shown in Figure 4E–H, SHP099 significantly increased the percentage of cells at the G0/G1 phase in *Ink4a/Arf*$^{-/-}$ mAsts and LN444 cells with expression of PDGFRα and/or PDGF-A compared with the cells expressing an empty vector. Additionally, SHP099 significantly increased cell apoptosis in *Ink4a/Arf*$^{-/-}$ mAsts with or without overexpression of PDGFRα/PDGF-A (Supplementary Figure 2A and 2B). This observation was validated in GSC 157 cells with endogenous PDGFRα activation. SHP099 inhibited levels of *JUN* mRNA expression (Supplementary Figure 3A) and significantly increased the percentage of cells at the G0/G1 phase (Supplementary Figure 3B and 3C) in GSC 157 cells. These data suggest that SHP099 specifically inhibits cell cycle pathways in glioma cells with PDGFRα activation.

SHP099 Reaches the Brains of Immunocompetent Animals at an Efficacious Concentration

A major challenge for agents targeting gliomas is their ability to cross the blood–brain barrier (BBB) and reach effective concentrations within the tumor.[33] Most chemotherapeutic and targeted agents are unable to effectively cross the BBB, thereby resulting in their failure to suppress GBM tumorigenicity.[34] Thus, we assessed the ability of SHP099 to cross the BBB in C57BL/6J mice after oral gavage of a single dose of SHP099 at 100 mg/kg in a volume of 400 μL. Brain tissue and plasma samples were collected at indicated time points and analyzed by UHPLC-MS to measure SHP099 kinetics. The ion spectrums of UHPLC-MS analysis of SHP099 in plasma and brain tissues at 4 h post oral gavage in mice were shown (Supplementary Figure 4). The concentrations of SHP099 were higher in plasma and brain tissues at the early time points after oral gavage (Figure 5A); and at 24 h post oral gavage, levels of SHP099 remained at an appreciable level in brain tissue (Figure 5A). The brain–plasma ratio was >1 at the time points from 1 h to 24 h (Supplementary Table 3), indicating that SHP099 reaches the brains of animals at an efficacious concentration in the time similar to SHP099 in the circulation/plasma.

Fig. 4 SHP099 specifically inhibits cell cycle pathways in glioma cells with PDGFRα activation. (A) Heatmap of RNA-Seq analysis of differentially expressed genes (2-fold change and false discovery rate < 0.05) in *Ink4a/Arf*$^{-/-}$ mAsts with ectopic expression of PDGFRα and PDGF-A treated with 0, 5, or 10 μM SHP099 in duplicate samples. (B) Expression of *JUN* after SHP099 treatment using RNA-Seq (left) and qRT-PCR (right) assays. (C) Gene Ontology analysis indicated that genes downregulated by SHP099 were associated with cell cycle pathways. (D) GSEA of SHP099-inhibited pathways using ranked gene expression changes in *Ink4a/Arf*$^{-/-}$ mAsts with ectopic expression of PDGFRα and PDGF-A treated with 5 or 10 μM SHP099 compared with a vehicle control (0 μM SHP099). NES, normalized enrichment score. (E and G) Representative images from flow cytometric analysis of the influence of SHP099 treatment on cell cycle in *Ink4a/Arf*$^{-/-}$ mAsts with ectopic expression of PDGFRα and PDGF-A (E) or LN444 cells with ectopic expression of an EV or PDGF-A (G). (F and H) Percentage of cells in G0/G1 phase in (E) and (G), respectively. *$P < 0.05$, **$P < 0.01$, ***$P < 0.001$, by one-way ANOVA.

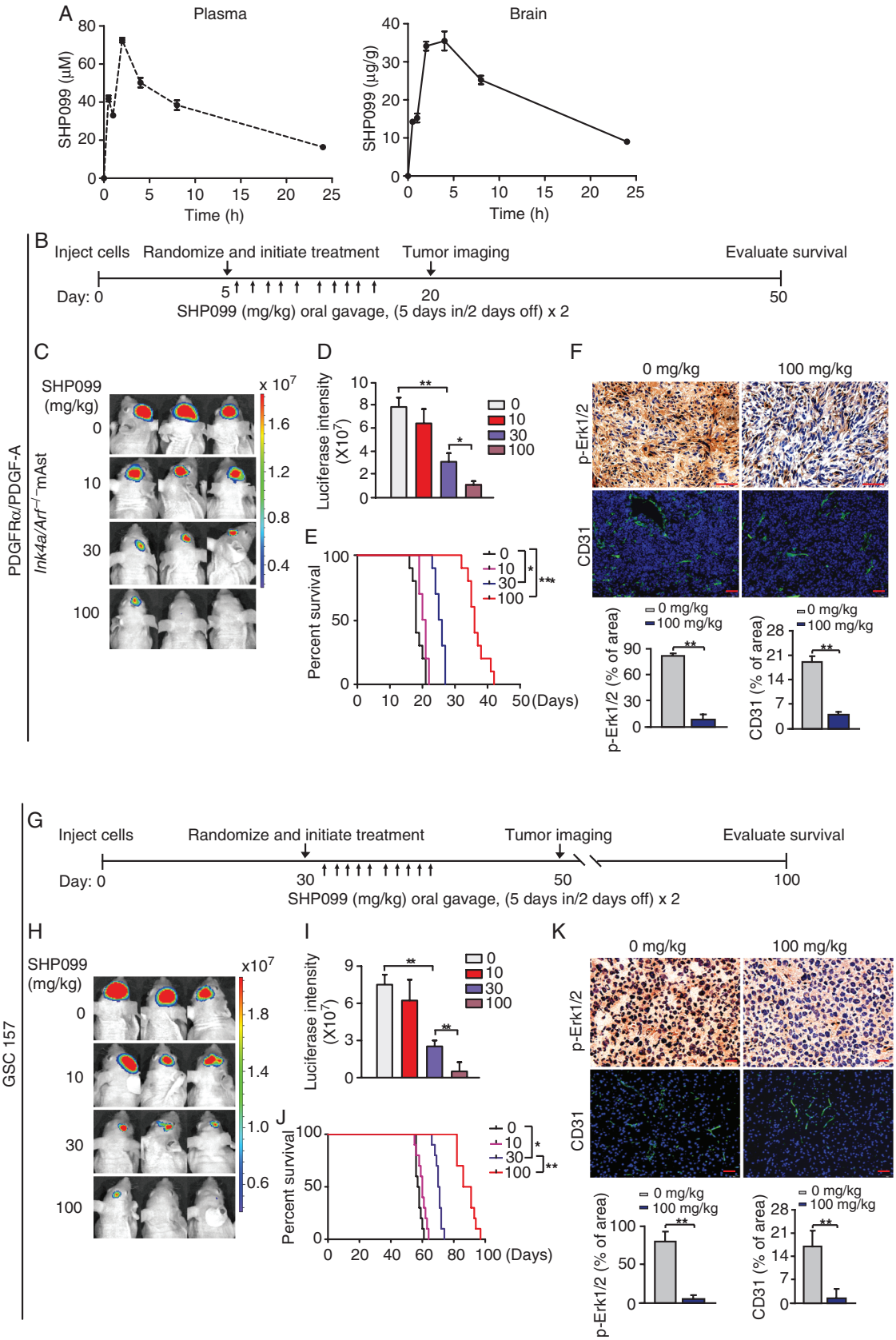
A
Plasma
SHP099 (μM)
Time (h)
Brain
SHP099 (μg/g)
Time (h)
B
Inject cells
Randomize and initiate treatment
Tumor imaging
Evaluate survival
Day: 0
5
20
50
SHP099 (mg/kg) oral gavage, (5 days in/2 days off) x 2
C
PDGFRα/PDGF-A
Ink4a/Arf−/−mAst
SHP099 (mg/kg)
0
10
30
100
x 10^7
1.6
1.2
0.8
0.4
D
Luciferase intensity (X10^7)
0
10
30
100
E
Percent survival
Days
F
0 mg/kg
100 mg/kg
p-Erk1/2
CD31
p-Erk1/2 (% of area)
CD31 (% of area)
G
Inject cells
Randomize and initiate treatment
Tumor imaging
Evaluate survival
Day: 0
30
50
100
SHP099 (mg/kg) oral gavage, (5 days in/2 days off) x 2
GSC 157
H
SHP099 (mg/kg)
x10^7
1.8
1.4
1.0
0.6
I
Luciferase intensity (X10^7)
J
Percent survival
Days
K
p-Erk1/2
CD31
p-Erk1/2 (% of area)
CD31 (% of area)

SHP099 as a Single Agent Inhibits PDGFRα-Driven Glioma Tumor Growth

To examine the in vivo antitumor effect of SHP099, we employed an orthotopic xenograft model in immunodeficient mice. *Ink4a/Arf*$^{-/-}$ mAsts with stable expression of PDGFRα/PDGF-A and luciferase were transplanted into the brains of the mice. Oral gavage of SHP099 was initiated after randomization by bioluminescence imaging (BLI) flux values to ensure that tumors were of equal size in the treatment and control groups (Figure 5B). Quantitation of BLI showed a significant reduction in tumor burden after treatment with SHP099 (Figure 5C and 5D). Moreover, the inhibition of tumor growth by SHP099 was dose dependent (Figure 5D). Kaplan–Meier analysis of the mice injected with *Ink4a/Arf*$^{-/-}$ mAsts with stable expression of PDGFRα/PDGF-A showed significant improvement in the survival of the 30 mg/kg SHP099-treated cohort compared with the control cohort ($P < 0.05$) (Figure 5E). Treatment of 100 mg/kg SHP099 extended survival to a significantly greater extent than 30 mg/kg SHP099 treatment ($P < 0.01$) (Figure 5E). Consistent with these biological effects, IHC analysis revealed that SHP099 decreased p-ERK1/2 and tumor vascularity, as evidenced by CD31 immunostaining in vivo (Figure 5F).

Next, we further evaluated the efficacy of SHP099 in a patient-derived GSC xenograft animal model. GSC 157 cells with PDGFRα activation (Figure 1D)[14,24] were implanted intracranially into immunodeficient mice. Thirty days after implantation, mice bearing GSC 157 xenografts were randomized and treated with SHP099 (Figure 5G). After treatment with SHP099, quantitation of BLI revealed a significant inhibition of tumor growth in a dose-dependent manner (Figure 5H and 5I). Kaplan–Meier analysis also showed a significant improvement in the survival of the SHP099-treated cohort in a dose-dependent manner (Figure 5J). Additionally, IHC analysis showed that SHP099 markedly reduced p-ERK1/2 and tumor vascularity in GSC 157 xenograft tumors (Figure 5K). As a control, we also determined the effects of SHP099 on animal survival with mouse GL261 glioma tumor xenografts that do not have endogenous PDGFRα activation. As shown in Supplementary Figure 5A, compared with the control *Ink4a/Arf*$^{-/-}$ mAsts expressing PDGFRα/PDGF-A, there is minimal or no expression of PDGFRα, PDGF-A, and p-PDGFRα in mouse GL261 glioma cells. Importantly, treatment of SHP099 in animals bearing GL261 glioma xenografts did not display any inhibitory effects on GL261 tumor growth (Supplementary Figure 5B–D) and any benefit of the survival of animal bearing GL261 glioma xenografts (Supplementary Figure 5E). These data support our hypothesis that SHP099 extends survival as a single agent in brain GBM tumor xenografts with activated PDGFRα signaling.

SHP099 in Combination with TMZ Extends the Survival of GBM-Bearing Mice

Adjuvant administration of TMZ, an alkylating agent, is the standard of care first-line treatment of GBM. To examine whether SHP099 treatment enhances antitumor activity of TMZ in vivo, we treated mice bearing *Ink4a/Arf*$^{-/-}$ mAst tumor xenografts that expressed PDGFRα/PDGF-A or GSC 157 tumor xenografts with SHP099 (100 mg/kg), TMZ (8 mg/kg) in combination, or a vehicle.[35] After randomization by BLI, oral gavage of SHP099 and intraperitoneal injection of TMZ were initiated (Figure 6A and 6E). At day 20 (*Ink4a/Arf*$^{-/-}$ mAsts) or day 50 (GSC 157) post implantation, all GBM tumor xenografts showed an increase at various levels in growth (Figure 6C and 6G), suggesting that treatment of SHP099, TMZ, or in combination with TMZ attenuated tumor growth but did not cause tumor regression. Compared with the vehicle control or TMZ, GBM tumor xenografts exposed to SHP099 or SHP099 in combination with TMZ exhibited significant inhibition in tumor growth (Figure 6B, C and Figure 6F, G). However, SHP099 in combination with TMZ significantly extended survival to a greater extent than SHP099 treatment alone (Figure 6D and 6H), indicating that the combination of SHP099 with TMZ synergizes to extend the survival in our GBM xenograft models.

Discussion

Despite extensive efforts via surgery resection and adjuvant therapies over the past decades, the prognosis of patients with GBM remains dismal. Hence, there is a critical need for the development of effective therapies for GBM. In this study, we conducted an extensive preclinical in vitro and in vivo analysis of SHP099 inhibition of multiple GSC cells and 2 GBM xenograft models. GSCs were more responsive to SHP099 compared with NPCs in vitro. SHP099 accumulated at efficacious concentrations in the brain to inhibit ERK1/2 activation in vivo and extended the survival of mice as a single agent or in combination with TMZ in orthotopic GBM xenografts.

In this study, we demonstrate that SHP099 is a potent, selective, orally efficacious SHP-2 inhibitor against GBM.

Fig. 5 SHP099 can effectively cross the BBB and inhibits PDGFRα-driven glioma tumor growth as a single agent. (A) Pharmacokinetics of SHP099 in plasma and brain tissue of immunocompetent mice. Six-week-old C57BL/6J female mice were administered by oral gavage a single dose of SHP099 (100 mg/kg in a total volume of 400 μL). Brain tissue and plasma were harvested at indicated time points post oral gavage (0 min, 30 min, 1 h, 2 h, 4 h, 8 h, and 24 h) and subjected to UHPLC-MS analysis. Three mice were used for each point. See also Supplementary Table 3B and G) Treatment schemes for the evaluation of in vivo efficacy of SHP099 in *Ink4a/Arf*$^{-/-}$ mAst (B) or GSC 157 (G) xenografts. Animals were treated with the indicated SHP099 doses from Monday to Friday within 2 weeks. (C and D) Representative images (C) at day 20 and quantitation of BLI (D) of *Ink4a/Arf*$^{-/-}$ mAst xenografts with ectopic expression of PDGFRα and PDGF-A from SHP099 treated and control mice. (E) Kaplan–Meier survival analysis of animals with *Ink4a/Arf*$^{-/-}$ mAst tumors ($n = 10$ per group). (F) Upper panel, representative images of IHC analysis of xenografts in C using anti-p-ERK1/2 and anti-CD31 antibodies. Lower panel, quantitation of p-ERK1/2 and CD31 positive cells. (H, I) Representative images at day 50 (H) and quantitation of BLI (I) of GSC 157 xenografts from SHP099 treated and control mice. (J) Kaplan–Meier survival analysis of mice with GSC 157 tumors ($n = 10$ per group). (K) Representative images of IHC analysis of xenografts in H using anti-p-ERK1/2 and anti-CD31 antibodies. Lower, quantitation of p-ERK1/2 and CD31 positive cells. In F and K, scale bars, 50 μm. *$P < 0.05$, **$P < 0.01$, by two-tailed Student's *t*-test or log-rank analysis.

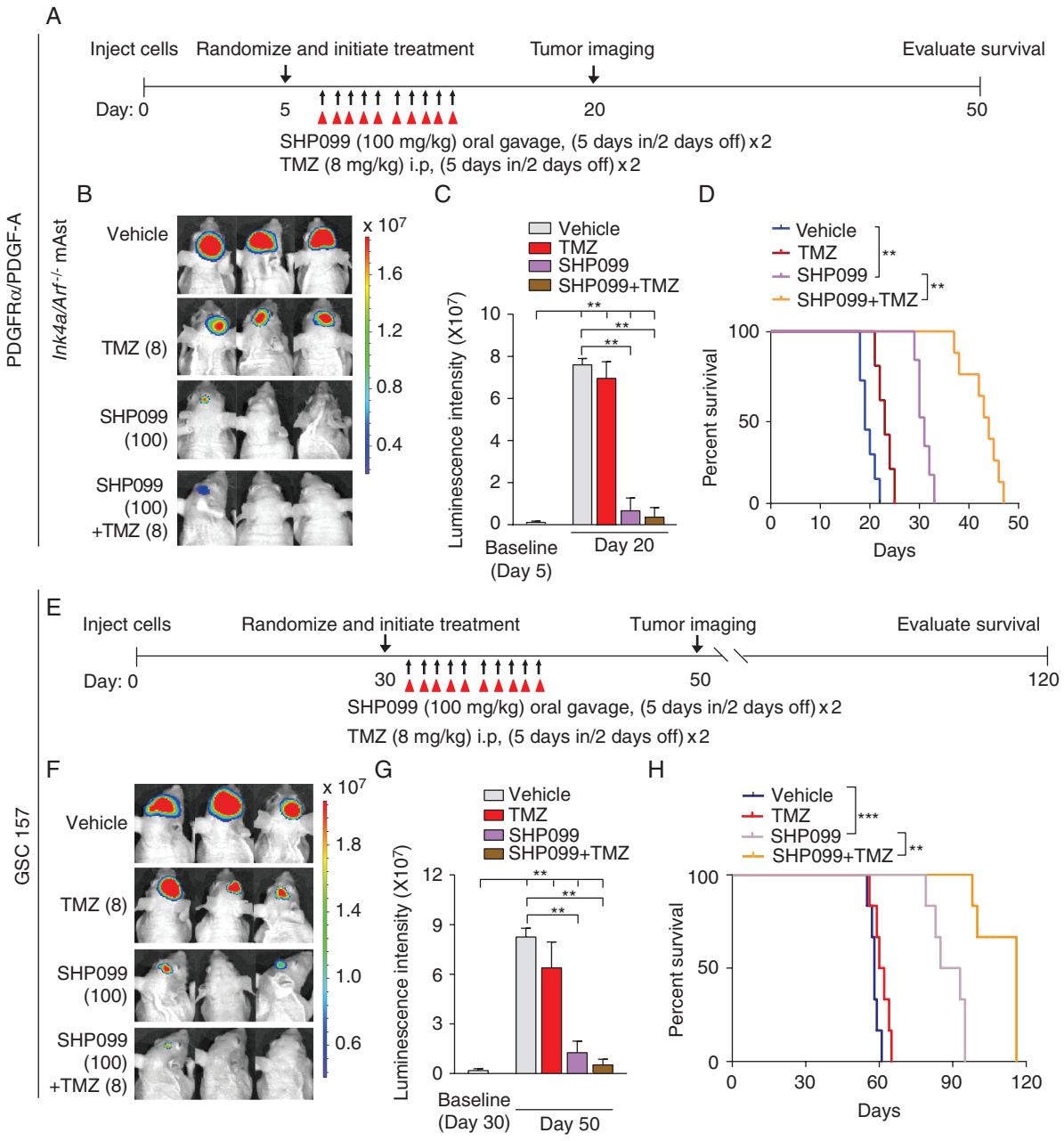

Fig. 6 SHP099 in combination with TMZ extends the survival of GBM-bearing animal. (A and E) Treatment scheme for the evaluation of in vivo efficacy of SHP099 in combination with TMZ in *Ink4a/Arf*$^{-/-}$ mAsts (A) or GSC 157 (E) tumor xenografts. The mice were treated with indicated 100 mg/kg SHP099 with or without 8 mg/kg TMZ from Monday to Friday within 2 weeks. (B and C) Representative images (B) on day 20 and quantitation of BLI at the indicated date (C) of *Ink4a/Arf*$^{-/-}$ mAst xenografts with ectopic expression of PDGFRα and PDGF-A from SHP099 treated and control mice. (D) Kaplan–Meier survival analysis of animals with *Ink4a/Arf*$^{-/-}$ mAst tumors ($n = 10$ per group). (F and G) Representative images on day 50 (F) and quantitation of BLI at the indicated date (G) of GSC 157 tumor xenografts from SHP099 treated and control mice. (H) Kaplan–Meier survival analysis of mice with GSC 157 tumor xenografts ($n = 6$ per group). $^{**}P < 0.01$, $^{***}P < 0.001$, by two-tailed Student's *t*-test, one-way ANOVA, or log-rank analysis.

SHP-2 was the first reported PTP[36] and is dysregulated in multiple diseases,[37] including glioma.[13] SHP-2 inhibitors (NSC-87877, IIB-08, GS-493, and IIa-1) have substantiated in vitro potency, PTP selectivity, and beneficial effects in animal models.[38] In particular, IIB-08 was previously shown to effectively suppress the growth of orthotopic GBM xenografts.[12] However, these SHP-2 inhibitors have still not been reported to be efficacious for clinical GBM treatment. In this study, we showed that similar to IIB-08, SHP099 preferentially inhibited cell proliferation of GBM and GSCs in vitro and was able to cross the BBB to inhibit SHP-2 activity and the growth of orthotopic GBM

xenografts. Additionally, several studies reported SHP099 as a more promising agent for clinical treatment compared with IIB-08. First, IIB-08 is an indolo-salicylic acid compound and targets both the active site and an adjacent peripheral site of SHP-2,[39] whereas SHP099 binds to a heretofore unrecognized pocket in "closed" SHP-2, acting like "molecular glue" to prevent N-SH2/loop/C-SH2 movements that presumably occur upon enzyme activation.[18] Second, IIB-08 inhibited p-nitrophenyl phosphate hydrolysis at a dissociation constant (K_d) of 5.5 μM,[39] whereas SHP099 exhibited SHP-2 inhibitory activity (IC_{50} = 71 nM).[18] Third, SHP099 displayed minimal activity against a panel of other PTPs (including SHP-1) and kinases.[18] In contrast, IIB-08 was shown to inhibit SHP-1 activity.[39] Fourth, this study and another report[18] showed that SHP099 did not inhibit RTK-activated Akt phosphorylation, whereas IIB-08 reduced RTK-activated Akt phosphorylation.[12] Finally, consistent with a previous report,[19] in this study our data demonstrated that SHP099 is orally bioavailable.

The protective function of the BBB poses a major challenge for small-molecule inhibitors and other therapeutic agents in terms of effective treatment of brain tumors. Although our data could not provide direct evidence to support the conclusion that SHP099 penetrates the BBB in the brain of animals, our data did provide indicative evidence that SHP099 reaches the brains of animals at an efficacious concentration in a time similar to SHP099 in the circulation/plasma. Moreover, our vivo data showing that SHP099 effectively inhibited GBM brain tumor xenograft tumorigenicity strongly suggest that SHP099 reaches the brain tumor xenograft beds and exhibits the inhibitory effects on tumor growth in the brain of animals.

Although the prevalence of PDGFRα activation/amplification is at a relatively lower frequency in clinical GBM compared with EGFR amplification, PDGFRα amplifications occur in approximately 13% of GBM and are enriched in proneural subtype tumors.[16] Moreover, the majority of gliomas, particularly those with an oligodendrocyte cell of origin, have aberrant PDGFR signaling, which can be used in conjunction with EGFR to classify gliomas.[40] Here, our results showed that PDGF-A stimulation enhanced SHP099 response in GSCs with endogenously high PDGFRα activation/amplification or GBM cells with ectopic expression of PDGFRα and/or PDGF-A. Thus, our findings suggest the clinical utility of SHP-2 inhibition as a targeted therapy approach for RTK-driven GBM.

Genetic and biochemical analyses have established that SHP-2 blocks ERK1/2 phosphorylation and proliferation of various cells driven by aberrantly activated RTKs. However, the mechanism by which SHP099 selectively inhibits RTK-driven cell proliferation remains unclear. In this study, our data not only validate the critical roles of SHP-2–ERK1/2 in glioma proliferation and survival, but also provide evidence that the observed effects reflect specific SHP099 inhibition for SHP-2 in GBM. Moreover, we showed that SHP099 specifically suppressed the expression of a signaling factor, *JUN*, downstream of PDGFRα in GBM, thereby inducing G1 phase cell cycle arrest. To the best of our knowledge, this is the first study to reveal that SHP099 impairs cell cycle.

Taken together, this study is the first to determine the preclinical activity of SHP099 against GBM with activated PDGFRα signaling and to assess its potential as an antitumor agent. Our data not only demonstrate that SHP099 effectively inhibits PDGFRα-driven GBM tumor xenograft growth in the brains of animals but also reveal that SHP099 is a potent, selective, orally efficacious SHP-2 inhibitor against GBM. Moreover, SHP099 as a single agent or in combination with TMZ provides significant survival benefits to GBM tumor xenograft-bearing animals. These results provide a strong rationale for validation of combination of SHP099 and TMZ as a therapeutic approach against GBM.

Supplementary Material

Supplementary data are available at *Neuro-Oncology* online.

Keywords

cell cycle | glioma stem-like cell | PDGFRα | SHP-2 | SHP099

Funding

This work was supported in part by National Natural Science Foundation of China (no. 81572467, 81874078 to H. Feng; no. 81772663 to Y. Li; no. 81703533 to W. Zhang); the Program for Professor of Special Appointment (Eastern Scholar) at Shanghai Institutions of Higher Learning (no. 2014024), Shanghai Municipal Education Commission-Gaofeng Clinical Medicine Grant Support (no. 20161310), New Hundred Talent Program (Outstanding Academic Leader) at Shanghai Municipal Health Bureau (2017BR021), and the State Key Laboratory of Oncogenes and Related Genes in China (no. 91-17-25) to H. Feng; Shanghai Natural Science Foundation (16ZR1420200) and Shanghai Jiao Tong University Medical Engineering Cross Fund (YG2015QN35) to W. Zhang; Cultivation fund of Renji Hospital (PYIII-17–024) to Y. Hou; the Doctoral Innovation Fund Projects from Shanghai Jiao Tong University, School of Medicine (BXJ201819) to Y. Sang; funds from the Lou & Jean Malnati Brain Tumor Institute of Northwestern Medicine to S-Y. Cheng.

Acknowledgments

We thank Ichiro Nakano for providing patient-derived glioma spheres and Erwin G. Van Meir for providing LN444 cells.

Conflict of interest statement. All authors declare no conflict of interest.

Authorship statement. WZ, YL, and HF designed and supervised the project. YS, YH, RC, LZ, and WZ performed experiments. YS, YH, WZ, YL, and HF interpreted and/or reviewed the data. YS, YH, LZ, AAA, BH, S-YC, WZ, YL, and HF wrote or edited the manuscript.

References

1. Osuka S, Van Meir EG. Overcoming therapeutic resistance in glioblastoma: the way forward. *J Clin Invest.* 2017;127(2):415–426.
2. Wen PY, Kesari S. Malignant gliomas in adults. *N Engl J Med.* 2008;359(5):492–507.
3. Huang T, Kim CK, Alvarez AA, et al. MST4 phosphorylation of ATG4B regulates autophagic activity, tumorigenicity, and radioresistance in glioblastoma. *Cancer Cell.* 2017;32(6):840–855 e848.
4. Polson ES, Kuchler VB, Abbosh C, et al. KHS101 disrupts energy metabolism in human glioblastoma cells and reduces tumor growth in mice. *Sci Transl Med.* 2018;10(454):1–12.
5. Canella A, Welker AM, Yoo JY, et al. Efficacy of onalespib, a long-acting second-generation HSP90 inhibitor, as a single agent and in combination with temozolomide against malignant gliomas. *Clin Cancer Res.* 2017;23(20):6215–6226.
6. Krzyzosiak A, Sigurdardottir A, Luh L, et al. Target-based discovery of an inhibitor of the regulatory phosphatase PPP1R15B. *Cell.* 2018;174(5):1216–1228.e19.
7. Freeman RM Jr, Plutzky J, Neel BG. Identification of a human src homology 2-containing protein-tyrosine-phosphatase: a putative homolog of Drosophila corkscrew. *Proc Natl Acad Sci U S A.* 1992;89(23):11239–11243.
8. Tajan M, de Rocca Serra A, Valet P, Edouard T, Yart A. SHP2 sails from physiology to pathology. *Eur J Med Genet.* 2015;58(10):509–525.
9. Huang WQ, Lin Q, Zhuang X, et al. Structure, function, and pathogenesis of SHP2 in developmental disorders and tumorigenesis. *Curr Cancer Drug Targets.* 2014;14(6):567–588.
10. Dance M, Montagner A, Salles JP, Yart A, Raynal P. The molecular functions of Shp2 in the Ras/mitogen-activated protein kinase (ERK1/2) pathway. *Cell Signal.* 2008;20(3):453–459.
11. Zhang J, Zhang F, Niu R. Functions of Shp2 in cancer. *J Cell Mol Med.* 2015;19(9):2075–2083.
12. Bunda S, Burrell K, Heir P, et al. Inhibition of SHP2-mediated dephosphorylation of Ras suppresses oncogenesis. *Nat Commun.* 2015;6:8859.
13. Liu KW, Feng H, Bachoo R, et al. SHP-2/PTPN11 mediates gliomagenesis driven by PDGFRA and INK4A/ARF aberrations in mice and humans. *J Clin Invest.* 2011;121(3):905–917.
14. Zhang L, Zhang W, Li Y, et al. SHP-2-upregulated ZEB1 is important for PDGFRα-driven glioma epithelial-mesenchymal transition and invasion in mice and humans. *Oncogene.* 2016;35(43):5641–5652.
15. The Cancer Genome Atlas Research Network. Comprehensive genomic characterization defines human glioblastoma genes and core pathways. *Nature.* 2008;455(7216):1061–1068.
16. Verhaak RG, Hoadley KA, Purdom E, et al. Integrated genomic analysis identifies clinically relevant subtypes of glioblastoma characterized by abnormalities in PDGFRA, IDH1, EGFR, and NF1. *Cancer Cell.* 2010;17(1):98–110.
17. Noel LA, Arts FA, Montano-Almendras CP, et al. The tyrosine phosphatase SHP2 is required for cell transformation by the receptor tyrosine kinase mutants FIP1L1-PDGFRalpha and PDGFRalpha D842V. *Mol Oncol.* 2014;8(3):728–740.
18. Chen YN, LaMarche MJ, Chan HM, et al. Allosteric inhibition of SHP2 phosphatase inhibits cancers driven by receptor tyrosine kinases. *Nature.* 2016;535(7610):148–152.
19. Garcia Fortanet J, Chen CH, Chen YN, et al. Allosteric inhibition of SHP2: identification of a potent, selective, and orally efficacious phosphatase inhibitor. *J Med Chem.* 2016;59(17):7773–7782.
20. Fedele C, Ran H, Diskin B, et al. SHP2 inhibition prevents adaptive resistance to MEK inhibitors in multiple cancer models. *Cancer Discov.* 2018;8(10):1237–1249.
21. Ruess DA, Heynen GJ, Ciecielski KJ, et al. Mutant KRAS-driven cancers depend on PTPN11/SHP2 phosphatase. *Nat Med.* 2018;24(7):954–960.
22. Mainardi S, Mulero-Sánchez A, Prahallad A, et al. SHP2 is required for growth of KRAS-mutant non-small-cell lung cancer in vivo. *Nat Med.* 2018;24(7):961–967.
23. Wong GS, Zhou J, Liu JB, et al. Targeting wild-type KRAS-amplified gastroesophageal cancer through combined MEK and SHP2 inhibition. *Nat Med.* 2018;24(7):968–977.
24. Mao P, Joshi K, Li J, et al. Mesenchymal glioma stem cells are maintained by activated glycolytic metabolism involving aldehyde dehydrogenase 1A3. *Proc Natl Acad Sci U S A.* 2013;110(21):8644–8649.
25. Bachoo RM, Maher EA, Ligon KL, et al. Epidermal growth factor receptor and Ink4a/Arf: convergent mechanisms governing terminal differentiation and transformation along the neural stem cell to astrocyte axis. *Cancer Cell.* 2002;1(3):269–277.
26. Lv D, Li Y, Zhang W, et al. TRIM24 is an oncogenic transcriptional co-activator of STAT3 in glioblastoma. *Nat Commun.* 2017;8(1):1454.
27. Subramanian A, Tamayo P, Mootha VK, et al. Gene set enrichment analysis: a knowledge-based approach for interpreting genome-wide expression profiles. *Proc Natl Acad Sci U S A.* 2005;102(43):15545–15550.
28. Parsons DW, Jones S, Zhang X, et al. An integrated genomic analysis of human glioblastoma multiforme. *Science.* 2008;321(5897):1807–1812.
29. Feng H, Hu B, Liu KW, et al. Activation of Rac1 by Src-dependent phosphorylation of Dock180(Y1811) mediates PDGFRα-stimulated glioma tumorigenesis in mice and humans. *J Clin Invest.* 2011;121(12):4670–4684.
30. Rosenkranz S, DeMali KA, Gelderloos JA, Bazenet C, Kazlauskas A. Identification of the receptor-associated signaling enzymes that are required for platelet-derived growth factor-AA-dependent chemotaxis and DNA synthesis. *J Biol Chem.* 1999;274(40):28335–28343.
31. Klinghoffer RA, Hamilton TG, Hoch R, Soriano P. An allelic series at the PDGFalphaR locus indicates unequal contributions of distinct signaling pathways during development. *Dev Cell.* 2002;2(1):103–113.
32. Wisdom R, Johnson RS, Moore C. c-Jun regulates cell cycle progression and apoptosis by distinct mechanisms. *EMBO J.* 1999;18(1):188–197.
33. Lapointe S, Perry A, Butowski NA. Primary brain tumours in adults. *Lancet.* 2018;392(10145):432–446.
34. Pardridge WM. The blood-brain barrier: bottleneck in brain drug development. *NeuroRx.* 2005;2(1):3–14.
35. Blakeley JO, Grossman SA, Chi AS, et al. Phase II study of iniparib with concurrent chemoradiation in patients with newly diagnosed glioblastoma. *Clin Cancer Res.* 2019;25(1):73–79.
36. Chan RJ, Feng GS. PTPN11 is the first identified proto-oncogene that encodes a tyrosine phosphatase. *Blood.* 2007;109(3):862–867.
37. He RJ, Yu ZH, Zhang RY, Zhang ZY. Protein tyrosine phosphatases as potential therapeutic targets. *Acta Pharmacol Sin.* 2014;35(10):1227–1246.
38. Tsutsumi R, Ran H, Neel BG. Off-target inhibition by active site-targeting SHP2 inhibitors. *FEBS Open Bio.* 2018;8(9):1405–1411.
39. Zhang X, He Y, Liu S, et al. Salicylic acid based small molecule inhibitor for the oncogenic Src homology-2 domain containing protein tyrosine phosphatase-2 (SHP2). *J Med Chem.* 2010;53(6):2482–2493.
40. Sun Y, Zhang W, Chen D, et al. A glioma classification scheme based on coexpression modules of EGFR and PDGFRA. *Proc Natl Acad Sci U S A.* 2014;111(9):3538–3543.